haematologica
Journal of The Ferrata Storti Foundation

Mesenchymal stromal cells confer chemoresistance to myeloid leukemia blasts through Side Population functionality and ABC transporter activation

by Laetitia Boutin, Pierre Arnautou, Aurélie Trignol, Amandine Ségot, Thomas Farge, Christophe Desterke, Sabrina Soave, Denis Clay, Emmanuel Raffoux, Jean-Emmanuel Sarry, Jean-Valère Malfuson, Jean-Jacques Lataillade, Marie-Caroline Le Bousse-Kerdilès, and Adrienne Anginot

Haematologica 2019 [Epub ahead of print]

Citation: Laetitia Boutin, Pierre Arnautou, Aurélie Trignol, Amandine Ségot, Thomas Farge, Christophe Desterke, Sabrina Soave, Denis Clay, Emmanuel Raffoux, Jean-Emmanuel Sarry, Jean-Valère Malfuson, Jean-Jacques Lataillade, Marie-Caroline Le Bousse-Kerdilès, and Adrienne Anginot. Mesenchymal stromal cells confer chemoresistance to myeloid leukemia blasts through Side Population functionality and ABC transporter activation. Haematologica. 2019; 104:xxx doi:10.3324/haematol.2018.214379

Mesenchymal stromal cells confer chemoresistance to myeloid leukemia blasts through Side Population functionality and ABC transporter activation

Laetitia Boutin[1,2], Pierre Arnautou[3], Aurélie Trignol[1], Amandine Ségot[3], Thomas Farge[4], Christophe Desterke[5], Sabrina Soave[2], Denis Clay[5], Emmanuel Raffoux[6], Jean-Emmanuel Sarry[4], Jean-Valère Malfuson[3,2], Jean-Jacques Lataillade[1,2], Marie-Caroline Le Bousse-Kerdilès[2,*] and Adrienne Anginot[2,*]

[1] CTSA, IRBA, Rue Raoul Batany, Clamart, France.

[2] Inserm UMR-S-MD1197, Paul Brousse Hospital, Paris 11 University, Villejuif, France.

[3] Service d'hématologie, HIA Percy, Clamart, France

[4] Inserm U1037, Cancer Research Center of Toulouse, University of Toulouse, Toulouse, France

[5] Inserm UMS33, Paul Brousse Hospital, Paris 11 University, Villejuif, France.

[6] Service d'hématologie adulte, Saint louis Hospital, Paris, France

* AA and MCLBK contributed equally to this work

Running title: MSC-induced SP phenotype leads to chemoresistance

Keywords: Side population, chemoresistance, mesenchymal stromal cells, acute myeloid leukemia, detoxification signature

Abstract

Targeting chemoresistant malignant cells is one of the current major challenges in oncology. Therefore, it is mandatory to refine the characteristics of these cells to monitor their survival and develop adapted therapies. This is particularly of interest for acute myeloid leukemia for which 5-year survival rate reach only 30% for all prognosis. The role of microenvironment is increasingly reported to be a key regulator for blast survival. In this context, we demonstrate that contact with mesenchymal stromal cells promote a better survival of blasts in culture in presence of anthracycline through the activation of ABC transporters. Stroma-dependent ABC transporter activation leads to the induction of a side population phenotype in a subpopulation of primary leukemia blasts through Alpha4 engagement. The stroma-promoting effect is reversible and is observed with stromal cells isolated from either healthy donors or leukemia patients. Blasts expressing a side population phenotype are mostly quiescent and are chemoresistant *in vitro* and *in vivo* in patient-derived xenograft mouse models. At the transcriptomic level, blats from the side population are specifically enriched in drug metabolism program. This detoxification signature engaged in contact with mesenchymal stromal cells represents promising ways to target stroma-induced chemoresistance of acute myeloid leukemia cells.

Introduction

Acute myeloid leukemias (AMLs) represent a set of hemopathies characterized by a clonal expansion in bone marrow and blood of immature myeloid cells, called blasts, blocked at different stages of differentiation. AMLs can be classified according to immaturity degree (FAB classification) or depending upon the cytogenetic or molecular events observed in patients (OMS classification, 2016)[1]. AMLs are also subdivided in three groups conditioning the therapeutic care: favorable AMLs which may be cured without hematopoietic stem cell transplant, intermediate and adverse AMLs which may require an allogenic graft. Despite significant supportive care progresses, few medical discoveries radically changed AML prognosis since the 5-year survival rate is 30% for all groups of AMLs and 10% for adverse AMLs. The conventional chemotherapy based on the injection of a nucleoside analogue combined with an anthracycline is used to kill AML cells. However, many patients relapse mainly due to the persistence of rare chemoresistant AML cells able to re-initiate the disease, likely corresponding to leukemia stem cells (LSCs).

As a mirror of normal hematopoiesis, several studies reported a specific phenotype for LSCs or leukemia initiating cells. This issue generated heterogeneous results[2], nevertheless it was described that cells able to engraft *de novo* or after a secondary transplant were present in the $CD34^+CD38^-CD123^+$ hematopoietic population[3,4,5]. However, other studies showed that cells able to initiate leukemia concerned $CD34^-$, $CD33^+$ or $CD13^+$ cells[6]. Recently, Farge *et al.* demonstrated that chemoresistance was more related to a specific oxidative metabolism rather than to a level of progenitor/stem cell phenotype[7]. Moreover, the high oxidative phosphorylation status is associated with elevated fatty acid oxidation and high expression of CD36, a fatty acid translocase recently identified as a marker of a LSC sub-population[8].

Considering hematopoietic neoplasms, it is now mandatory to encompass environment factors to understand their development, resistance and dissemination. In adults, hematopoiesis develops in the bone marrow (BM) where a dialogue between hematopoietic stem /progenitor cells (HSPC) and the microenvironment including mesenchymal stromal cells (MSCs), extracellular matrix components and soluble factors[9,10], is critical for maintaining stem cell function and homeostasis. Such a protective microenvironment has been reported to be implicated in the stemness and chemoresistance of leukemia blasts at the origin of Environment Mediated-Drug Resistance (EM-DR) process, and specifically of the Cell Adhesion Mediated-Drug Resistance (CAM-DR) concept[8,11]. Quiescence as well as protection against environmental and drug aggressions are major characteristics of stem cells also characterized by the Side Population (SP) phenotype[12]. We have previously shown that whereas circulating HSPCs from heathy donors (HD) do not exhibit a SP phenotype, this functionality can be induced after co-culture with MSCs in a VLA4- and CD44-dependent manner[13]. Interestingly, this MSC-induced SP population is enriched in HSCs as shown by its engraftment in immunodeficient mice[13].

In the present work conducted on a cohort of 34 AML patients, we showed that MSCs activate ABC transporters in a subpopulation of primary blasts, resulting in the induction of a SP phenotype. SP blasts are mostly quiescent and exhibit a low ROS transcriptional pathway compared to non-SP (MP) blasts. Furthermore, they are capable to efflux chemotherapy agents *in vitro* in cultures as well as *in vivo* in patient-derived xenograft models treated by cytarabine, validating a higher chemoresistance of SP cells compared to their MP counterparts. Altogether, our results demonstrate that the stroma-induced SP functionality is a new mechanism of CAM-DR for AML blasts.

Methods

Preparation of primary AML cells

Peripheral blood samples were collected at Percy (Clamart, France) and Saint Louis (Paris, France) hospitals after the informed consent of patients in accordance with Declaration of Helsinki principles (IDRCB 2017-A02149-44, CPP 2017-juill.-14644 ND-1eravis, CNIL MR001). Patient cohort represents 34 patients with primary AML (Figure S1). Patients were untreated at the time of blood uptake. Blood mononuclear cells were isolated on density gradient (1.077g/mL) before freezing[13].

Co-culture of primary AML cells on mesenchymal stromal cells (MSC)

Primary AML mononuclear cells were plated at $2x10^5/cm^2$ in SynH (Abcell-Bio) supplemented with L-Glutamine, non-essential amino acids and 10% FBS for 3 or 4 days on confluent MSCs isolated from the BM of either AML patients (n=9) or HDs (n=5) (supplementary material). AML blasts were cultured without MSC feeders for controls. Transwell and neutralization experiments are described in supplemental material.

In some experiments, mitoxantrone (50nM; Sigma Aldrich) was added to the co-culture for 24 hours and cells were pre-treated or not with verapamil (50µM) for 2 hours before adding mitoxantrone and during mitoxantrone treatment.

At the end of co-cultures, non-adherent cells were flushed and stained with anti-CD45 antibody and annexin V (Invitrogen). Counting beads (CountBright, Life Technologie) were added to cell suspension to quantify cell populations by flow cytometry using Fortessa apparatus with Diva software (Becton Dickinson).

SP cell detection and characterization

Hoechst staining was performed as previously described[14,13] (supplementary material). After Hoechst incubation, cells were placed on ice and stained with anti-CD45 antibody and a viability dye. Flow cytometry analysis was carried out on BD Fortessa apparatus. CD45 staining was use to gate on AML blasts and to avoid stromal contamination for SP analysis.

Drug efflux: To analyze drug efflux concomitantly with SP cell detection, mitoxantrone (90nM) was added to the cell suspension during the last 30 min of Hoechst staining.

ABC transporter functionality

Specific probes for ABCB1 ($DioC_2(3)$), ABCC1 (CMFDA), and ABCG2 (Purpurin 18) were incubated during 30 min at 37°C after co-culture or during Hoechst staining. Cells were then stained with CD45 antibodies and with a viability dye as mentioned in Table S2.

Transcriptomic analysis

See supplementary material

Patient-derived xenograft (PDX) model

Patient-derived xenografts were achieved as previously described[7,15] (supplementary material) under French Institutional Animal Care and Use (Committee of "Midi-Pyrénées" region-France) approval.

Statistics

Raw data of each group were analyzed using R (3.3.3) and Rstudio (0.99.896) software's. The packages used were stats, coin and multcomp for tests. Graphic representations of data were made for each group using Prism 6 or R (3.3.3) software's (package ggplot2). Statistical

comparisons between groups on a single quantitative variable were run as follows: resampling tests were used for group *versus* group comparisons, pairing on AML donor levels or on AML MSC donor level. When multiple comparisons were used inside a single experiment, p-values were corrected using the Benjamini/Hochberg method. The significance threshold to accept a statistical difference for a test or group of tests was 0.05 and tests were bilateral unless stated. Data are expressed in median with 25%-75% interquartile intervals.

Results

Leukemia blasts cultivated on MSCs actively efflux chemotherapy drugs by activating ABC transporters

We first characterized MSCs isolated from the BM of AML patients (AML MSCs) at diagnosis and compare them to MSCs isolated from BM of healthy donors (HD MSCs). Figure S2A shows that the number of cumulative population doubling was slower for AML MSCs than for HD MSCs. AML MSC clonogenicity was also weaker than that of HD MSCs (Figure S2B). Because AML MSCs were morphologically different from HD MSCs, we quantified senescent cells using β-galactosidase activity test. We observed that AML MSCs showed 5 to 10 times more senescent cells than HD MSCs as soon as passage 4 (Figure S2C). This result can explain the limited expansion capacity and clonogenicity of AML MSCs. Despite these growth alterations, no differences were observed regarding their phenotype ($CD45^-CD90^+CD73^+CD105^+$) (Figure S3A) or differentiation capacities since they were able to differentiate into adipocytes, osteoblasts, and chondrocytes similarly to HD MSCs (Figure S3B and C and supplementary material). We further analyzed their functional roles on AML blast survival by co-culturing blasts on either AML or HD MSCs. After a 3-day co-culture, cells were removed and blast viability was evaluated using Annexin V and 7AAD co-staining. Figure 1 shows that co-cultures with HD or AML MSCs significantly increases AML blast survival (Figure 1A left panel, $p=0.0004$, $n>12$). This difference was also observed when mitoxantrone, a chemotherapy drug, was added to co-cultures (Figure 1A right panel, $p=0.0003$, $n>12$).

To explain this increased survival, we evaluated the intracellular amount of mitoxantrone in the blast population co-cultivated with or without MSCs isolated from HDs or AML patients (Figure 1B). All blasts were positive for mitoxantrone after a 3-day culture without MSCs.

However, when blasts were co-cultivated in presence of MSCs either from HDs (Figure 1C) or AML patients (Figure 1D), the mitoxantrone Mean Fluorescent Intensity (MFI) was lower than that of blasts cultured without MSCs. This reduction was observed in most of the patients studied independently of the MSC origin (p=0.01, n=6 for HD MSCs and n=9 for AML MSCs).

Because blasts co-cultured on MSCs exhibit a lower intracellular amount of mitoxantrone compared to cells cultivated without MSCs, we studied by which mechanism the amount of intracellular mitoxantrone was reduced. It is now well known that ATP-binding cassette (ABC) transporters can efflux several molecules including chemotherapy drugs[16]. Therefore, we used specific probes such as $Dioc_2(3)$, CMFDA and purpurin18 to evaluate the activity of three main pump family's such as ABCB1 (MDR1), ABCC1 and ABCG2, respectively. Figure 2A shows a significant increase in the percentage of blasts that efflux the $Dioc_2(3)$ probe after a 3-day co-culture on HD MSCs (median 16.1% (12.8%) with MSCs *vs.* 6.18 (2%) without MSCs, p=0.005, n=9), demonstrating the implication of ABCB1 pump in this process. The Dioc2,3 MFI was also significantly decreased in AML blasts (p=0.02, n=9, Figure 2D). We also noticed an increase of ABCC1 and ABCG2 pump activities in a few number of AML patients (Figure 2B and C) but with no significant modulation of CMFDA and purpurin18 MFIs (Figure 2E and F). However, when activities of these three ABC transporters were analyzed individually, patient per patient, we observed that their activities were systematically modulated by MSC contact (except for one patient, AML 44; Figure S4) and that ABC transporters were differentially active from one patient to another. When blasts were co-cultured on MSCs isolated from AML patients, we observed an activation of the 3 ABC transporters (p=0.01, 0.02 and 0.008, respectively; n=3-9, Figure 2G to I) associated with a decrease of specific probe MFIs (p=0.01, n= 3-9; Figure 2 J, L), except for Dioc2,3 MFI which remained high (Figure 2J).

So, our results show that leukemia blasts demonstrate a specific pattern of ABC transporter activity that is modulated by contact with stromal cells in a patient-dependent manner. Moreover, the modulation of ABC transporter activities appears higher when blasts are co-cultivated with MSCs isolated from AML patients.

Leukemia blasts adopt a SP phenotype after close contact with MSCs through integrin interactions

ABC transporter activation is known to be involved in SP phenotype acquisition. We therefore analyzed the SP phenotype of blasts before and after co-culture with MSCs. Circulating blasts were gated on their SSC $CD45^{low}$ profile in flow cytometry (Figure 3A). In contrast to circulating Lin^- HSPCs freshly isolated from HDs[13], a small proportion of blasts (0.2%; interquartile 0.44%), isolated from about 50% of AML patients, expressed a SP phenotype before any stromal co-culture (Figure 3B). However, after a 3-day co-culture on HD MSCs, we observed for all AML patients that a SP population has emerged or was increased within blast cells with a median around 4% with an interquartile of 8.65% ($p<0.001$, n=27). We then analyzed whether co-culture with AML MSCs also induced or increased the percentage of circulating leukemia blasts with a SP phenotype. Figure 3C shows that, similarly to MSCs isolated from HDs, co-cultures of blasts with AML MSCs systematically increased the percentage of SP blasts ($p=10^{-4}$, n= 8-35).

We further studied whether a close contact between blasts and MSCs was required to promote the SP phenotype of blasts. We first addressed this question by analyzing the proportion of SP blasts in the adherent fraction of the co-cultures and compared it with that detected in the supernatants (SN). Figure 3D shows that SP expressing cells were mostly found in the adherent fraction. We then confirmed the requirement of cell-cell interactions using transwell experiments in which the percentage of SP blasts was strongly reduced when blasts and

stromal cells were separated by the transwell insert (n=3, Figure 3D and E). So, close contacts between leukemia and stromal cells are mandatory to promote the SP phenotype in blasts.

We previously demonstrated that SP phenotype induced on circulating Lin^- HSPCs from HDs by MSC co-culture was dependent of alpha4 and beta1 integrins as well as CD44 engagement[13]. Using blocking antibodies, we tested whether the promotion of SP phenotype on AML blasts was dependent of MSC interactions through these molecules. Figure 3F shows that blocking alpha4 integrin significantly reduced the percentage of SP blasts after MSC co-culture ($p=0.04$, $n=7$) while blocking beta1 integrin and CD44 interactions had a slight but not significant effect on this proportion. We then tested the effect of pharmacological inhibitors on the main signaling pathways directly or indirectly activated by integrins. In that purpose, we first assessed the efficient dose corresponding to the highest dose that didn't induce toxicity for Dasatinib (pSrc inhibitor), LY294002 (pAKT inhibitor), CAS2859863 (pSTAT5 inhibitor) and LY209031 (pGSK3 inhibitor), CPD22 (pILK inhibitor) and Simvastatine (HMG coA reductase inhibitor) (data not shown). We then added these inhibitors to co-cultures and quantified the proportion of blasts that have adopted a SP phenotype after a 3-day co-culture on HD MSCs. Whereas addition of CPD22 or Simvastatine didn't affect the percentage of SP blasts (data not shown), a significant decreased of SP blasts was observed when Src ($p=0.002$, $n=9$), AKT ($p=0.003$, $n=9$), Stat5 ($p=0.009$, $n=9$) and GSK3 ($p=0.01$, $n=6$) pathways were inhibited (Figure 3G). These data confirms that the stroma-induced SP functionality on AML blasts was partly dependent of integrin's interactions and especially of alpha 4 integrin activation.

SP AML blasts are quiescent and able to actively efflux chemotherapy through ABCB1 transporters

SP phenotype is reported to be linked to quiescence[12–14]. Therefore, we analyzed by flow cytometry the cell cycle phases of AML blasts expressing or not the SP phenotype (SP *vs.* non-SP population/MP for Main Population) after a 3-day co-culture on HD MSCs. As expected, SP blasts were in majority in G0 phase (median 76% (16.5%)) in contrast to MP blasts (median 33.45% (18.6%)) which were mainly in G1-S-G2-M phases (Figure 4A). In agreement with this result, gene set enrichment analysis performed with KEGG database on data obtained from transcriptomic experiments, comparing sorted SP *vs*. MP blasts, showed an important repression of cell cycle and DNA replication gene expression in SP as compared to MP cells (Figure 4B).

When cultivated on MSCs, circulating AML blasts acquire the capability to efflux mitoxantrone through ABC transporter activation (Figure 1B-C). We therefore analyzed whether the drug efflux was restricted to SP blasts. In that purpose, blasts which were co-cultivated on MSCs during 3 days were incubated with mitoxantrone for the last 30 minutes of Hoechst incubation. We showed that SP blasts had a lower amount of mitoxantrone compared to MP blasts (Figure 4C). Quantification of mitoxantrone MFI (Figure 4D) in the SP population (median 1584 (1545)) showed a 2-fold decrease compared to the MP one (median 3219 (1706)) ($p=0.0052$; $n=12$) for most of patients analyzed. We thus evaluated which ABC transporters were activated in SP *vs*. MP cells using specific probes. Figure 4E shows that, here again, the ABCB1 transporter was significantly more active in SP (MFI $Dioc_2(3)$ 239 (2422)) than in MP blasts (MFI $Dioc_2(3)$ 1298 (3182)) ($p=0.023$, $n=7$). In contrast, ABCG2 and ABCC1 did not appear to be involved in this process (data not shown).

Altogether, our results demonstrate that AML blasts adopting SP phenotype after contact with MSCs are quiescent and able to actively efflux chemotherapy agents through ABC transporters and, in particular, through ABCB1.

SP blasts are more *in vitro* and *in vivo* chemoresistant than MP cells and this chemoresistance can be partially reversed by ABC transporter inhibition

We first tested whether the SP phenotype induced by contact with MSCs conferred a better in *vitro* survival to leukemia blasts in presence of chemotherapy drugs. We thus co-cultured blasts and MSCs isolated from HDs or AML patients in the presence or not of mitoxantrone. After a 3-day co-culture, we quantified the absolute number of SP and MP blasts in both conditions and calculated the survival rate of SP and MP cells by dividing the absolute number of SP or MP cells in the treated cultures by their absolute numbers in the non-treated cultures. The survival rate of SP cells was significantly higher than that of MP cells ($p=0.041$; $n=30$) when leukemia blasts were co-cultivated on MSCs independently of their origin (Figure 5A) or based on their origin (Figure 5B).

We further compared the *in vivo* chemoresistance of SP vs. MP cells in NSG mice grafted with primary AML blasts (PDX model). Twelve weeks after engraftment, the presence of human $CD45^+$ leukemic cells in mice was controlled by blood analysis. Then, mice were daily treated with cytarabine during 5 days to reduce the human blast population[7]. Three days after treatment arrest, mice were euthanized and their BM was harvested. We estimated the cell chimerism and showed that human $CD45^+$ cells represented between 70 and 96% of the whole $CD45^+$ population (Figure 5C). We then quantified the absolute number of total human blasts and of SP *vs*. MP human blasts present in the mouse BM. As expected, the global number of human blasts was highly reduced by the cytarabine treatment compare to PBS injection. However, and more interestingly, the absolute number of blasts expressing the SP

functionality remained unchanged after cytarabine treatment on the contrary to that of MP blasts that was 5-fold reduced (Figure 5D). These results show that cytarabine was active *in vivo* on MP blasts but less, or no, active on SP blasts.

Altogether, our results suggest that SP blasts are more resistant than MP cells to chemotherapy agents both *in vitro* and *in vivo*.

We then analyzed whether the chemosensitivity of AML blasts could be restored after blocking ABC transporters. We previously showed that ABC transporter activities (modulated on blasts after contact with MSCs) were differentially active and were patient dependent (Figure S4). Thus, we use verapamil, a broad spectrum ABC transporter inhibitor, to inhibit the SP phenotype[12,13]. Figure 5E shows that addition of verapamil into AML blast and MSC co-cultures significantly reduced the percentage of blasts that efflux mitoxantrone ($p=0.05$, $n=5$) as well as in mitoxantrone MFI ($p=0.05$, $n=5$, Figure 5F). Furthermore, when co-cultures were treated with a non-toxic dose of verapamil, we also observed a significant reduction of the number of living blasts compared to that observed with mitoxantrone alone ($p=0.01$, $n=6$, Figure 5G), suggesting that blocking ABC transporters restores blast mitoxantrone chemosensitivity.

AML SP blasts exhibit a detoxification transcriptional signature

As SP blasts were more chemoresistant *in vitro* and *in vivo* than their MP counterparts, we analyzed their transcriptomic profiles to highlight a specific signature of these cells. In that purpose, we sorted SP *vs.* MP blasts from two AML patients after a 3-day co-culture on HD MSCs. A global transcriptomic analysis of sorted SP *vs.* MP AML blasts demonstrated an enrichment of genes implicated in detoxification program in SP cells. Indeed, using KEEG database, GSEA analysis showed that the expression of genes involved in xenobiotic and drug metabolism *via* cytochrome P450 or by other enzymes was up regulated in SP blasts (Figure

6A). Surprisingly, the expression of ABC transporter transcripts was not homogeneously differentially modulated in SP *vs.* MP cells (Figure S5), suggesting that, in our experimental conditions, SP phenotype induction is not associated with an increase of ABC transporter mRNA level at steady state, as already suggested in other studies[17] but mainly after drug exposure[18,19]. We also observed that, oxidative phosphorylation, fatty acid metabolism and reactive oxygen species pathway signatures of Hallmark database were enriched in MP blasts (Figure 6B). Surprisingly, while SP phenotype is a common feature of stem cells[12] and the $CD34^+$ $CD38^-$ SP blast population is enriched in cells with a $CD123^+$ stem phenotype (Figure S6) as compared to $CD34^+$ $CD38^-$ MP cells, the stem cell transcriptional signatures proposed by Eppert *et al.*[20] and Ng *et al.*[21] were preferentially observed in the AML MP population (Figure 6C).

Discussion

Chemoresistance of leukemia cells is one of the major challenges which hematologists have to face in order to cure AMLs. Therefore, a better understanding of this process constitutes the keystone of next generation therapies. It is now well admitted that bone marrow microenvironment is a key actor of leukemia development and resistance to treatment but the underlying mechanisms remain still unclear.

Our present study shows that MSCs that play a central role in BM stromal niches, sustain the survival and chemoresistance of AML blasts through the induction of a SP phenotype. This chemoresistance mechanism involves activation of ABC transporters, responsible for drug efflux, in a small proportion of leukemia cells after co-culture with MSCs. Whereas these transporters were not or poorly active in circulating blasts, interactions with stromal cells constantly increased the proportion of SP cells in the blast population. Interestingly, the ABC transporter activation pattern appears to be patient dependent. While MSC-induced ABC transporter activation is common to all types of AMLs, we didn't found any correlation between specific probe efflux and patient characteristics. However, because AML is an heterogeneous group of diseases, it should be necessary to increase the size of the patient cohort to bring out a potential correlation between ABC transporter activation patterns and AML types. Beside a limited expansion capacity and clonogenicity, the capacity of AML MSCs to promote SP phenotype on blasts was similar and even better than that of HS MSCs. This observation suggests that the BM stroma of patients may be adapted to promote blast protection/survival and supports the hypothesis of a specific crosstalk between pathological blasts and MSCs.

Previous data from our group have demonstrated that BM MSCs modulate the SP phenotype of HSCs from HDs[13]. In the present study, we show that they also control the induction of the

SP functionality on AML blasts. Interestingly, SP leukemic blasts are mostly found in the MSC-adherent fraction, suggesting that close contacts between blasts and stromal cells are required for SP phenotype induction. As for HD samples, this process is partially dependent on α4 integrin. However, in contrast to HDs, for half of the patients studied, this induction is not dependent, or at a lower level, on β1 integrin or CD44, two cell-surface glycoproteins known to be involved in BM niche HSC nesting. BM niches are reported to be crucial for HSC long-term maintenance[22–24] and SP cell quiescence[25]. In patients, we show that the proportion of quiescent blasts is higher in the stroma induced-SP cell population than in their MP counterparts. Quiescence is often related to chemoresistance as only proliferating cells are sensitive to anthracyclines or nucleoside analogues. In the current study, we show that SP blasts are more chemoresistant than MP cells, either *in vitro* or *in vivo* in PDX models. This result is ascertained by our data showing that sorted SP blasts express a specific transcriptomic profile focused on genes involved in drug and environment stress detoxification[16] known to participate in the chemoresistance process[26]. Therefore, SP cell detection could allow monitoring chemoresistant blasts during the course of the disease and, targeting stroma-blast interactions would reinitiate cell cycling and, consequently, blast sensitization to chemotherapy. As VLA4 and CD44 play a role in the stroma-induced SP phenotype in HD HSCs but only partially in AML blasts, it would be relevant to identify specific interactions between MSCs and blasts to specifically target leukemia cells. Deep analyses using transcriptomic and interactomic approaches[27] focused on MSCs, SP and MP cells from AML patients and HDs should highlight new pairs of exclusive interactors involved in stroma-blast interactions that would be promising druggable targets.

An important clinical concern is the quest for leukemia stem/initiating cells[28]. SP cells exhibit some features of stem cells since they are mostly in G0[12,14,25] and since their reactive oxygen species (ROS) level is low as compared to their MP counterparts[29]. In our study, the

transcriptomic analysis of SP AML blasts doesn't correlate with the 114 and 17 gene stemness signatures reported by Eppert *et al*. and Ng *et al.* respectively[20,21], suggesting that SP AML cells are not enriched in such stem cells. Interestingly, Farge *et al*.[7] and Boyd et al.[30] demonstrated that chemotherapy-resistant human AML cells are not necessarily enriched in leukemia stem cells but exhibit increased fatty-acid oxidation, high oxidative phosphorylation (OXPHOS) gene signature and upregulated CD36 expression. By associating a reduction of transcripts for oxidative phosphorylation, fatty acid metabolism and reactive oxygen species in SP as compared to MP blasts, our results are somewhat in agreement with those from Ye *at al.* suggesting that chemoresistance is not necessarily restricted to the leukemia stem cell compartment but rather could be associated to metabolic adaptations induced by their microenvironment[8].

By promoting a better survival of blasts, the stroma-induced SP functionality we identified in blasts could represent a new mechanism of CAM-DR. Whereas BM MSCs from HD or AML patients exhibit nearly similar survival and SP-promoting effects on blasts, preliminary results on four patients suggest that cultivating MSCs and blasts in autologous conditions would bring a supplemental advantage on blast survival and chemoresistance. This suggests that an intimate cross talk has been settled down *in vivo* between MSCs and blasts and has been conserved *in vitro*. Recently, Moschoi et al.[31] proposed that mitochondrial transfers from BM stromal cells to AML blasts provided them a protective effect following chemotherapy. Other communication modes like exosomes exchange, metabolite secretion, and nanotube formation could also be suggested to participate in this process and must be identified to disrupt the stroma-induced chemoresistance of AML blasts.

Induction of SP/chemoresistance phenotype on AML blasts represents a major interest for clinicians as ABC transporters implicated in drug/chemotherapy agent efflux could be targeted[32,33]. In that context, we have shown that mitoxantrone efflux and blast survival are

reversible *in vitro* by addition of verapamil. However, results from clinical trials using P-glycoprotein inhibitors in AML patients are discouraging[34,35]. Our data showing that the functionality of the main ABC transporters implicated in MDR[36] is promoted by blast-MSC interactions and that this process is patient-dependent suggest that it is time to revisit the role of ABC transporters in therapeutic failure with regard to personalized medicine[37,38].

In conclusion, our results show the critical role of stroma interactions in blast chemoresistance through SP phenotype promotion and ABC transporter activation. Therefore, targeting these interactions in combination with the development of new improved inhibitors of ABC transporter function[39] could be a talented therapeutic alternative.

Acknowledgements

We thank the molecular core facility of Cochin Institute for transcriptomic analysis. We are very grateful to the polyclinic of Blois and particularly to Dr Denis Burgot as well as all the orthopedic surgery staff for providing human bone marrow samples from hip replacement. We thank Dr Cedric Thépenier for the statistical analysis and sharpened advices. We also thank Pr Christophe Martinaud for blast analysis on blood smears.

This work was supported by grants from Association “Laurette Fugain” (ALF 2013/08) and Association “Vaincre le Cancer-Nouvelles Recherches Biomédicales”.

Conflict of interest: The authors declare no conflict of interest.

References

1. Arber DA, Orazi A, Hasserjian R, et al. The 2016 revision to the World Health Organization classification of myeloid neoplasms and acute leukemia. Blood. 2016;127(20):2391–2405.

2. Taussig DC, Miraki-Moud F, Anjos-Afonso F, et al. Anti-CD38 antibody-mediated clearance of human repopulating cells masks the heterogeneity of leukemia-initiating cells. Blood. 2008;112(3):568–575.

3. van Rhenen A, Feller N, Kelder A, et al. High stem cell frequency in acute myeloid leukemia at diagnosis predicts high minimal residual disease and poor survival. Clin Cancer Res. 2005;11(18):6520–6527.

4. Vergez F, Green AS, Tamburini J, et al. High levels of CD34+CD38low/−CD123+ blasts are predictive of an adverse outcome in acute myeloid leukemia: a Groupe Ouest-Est des Leucémies Aiguës et Maladies du Sang (GOELAMS) study. Haematologica. 2011;96(12):1792–1798.

5. Jordan CT, Upchurch D, Szilvassy SJ, et al. The interleukin-3 receptor alpha chain is a unique marker for human acute myelogenous leukemia stem cells. Leukemia. 2000;14(10):1777–1784.

6. Sarry J-E, Murphy K, Perry R, et al. Human acute myelogenous leukemia stem cells are rare and heterogeneous when assayed in NOD/SCID/IL2Rγc-deficient mice. J Clin Invest. 2011;121(1):384–395.

7. Farge T, Saland E, de Toni F, et al. Chemotherapy-Resistant Human Acute Myeloid Leukemia Cells Are Not Enriched for Leukemic Stem Cells but Require Oxidative Metabolism. Cancer Discov. 2017;7(7):716–735.

8. Ye H, Adane B, Khan N, et al. Leukemic stem cells evade chemotherapy by metabolic adaptation to an adipose tissue niche. Cell Stem Cell. 2016;19(1):23–37.

9. Shafat MS, Gnaneswaran B, Bowles KM, Rushworth SA. The bone marrow microenvironment - Home of the leukemic blasts. Blood Rev. 2017;31(5):277–286.

10. Tabe Y, Konopleva M. Leukemia Stem Cells Microenvironment. Adv Exp Med Biol. 2017;1041:19–32.

11. Cukierman E, Bassi DE. The mesenchymal tumor microenvironment. Cell Adhes Migr. 2012;6(3):285–296.

12. Goodell MA, Brose K, Paradis g, Conner AS, Mulligan RC. Isolation and functional properties of murine hematopoietic stem cells that are replicating in vivo. J Exp Med. 1996;183(4):1797–1806.

13. Malfuson J-V, Boutin L, Clay D, et al. SP/drug efflux functionality of hematopoietic progenitors is controlled by mesenchymal niche through VLA-4/CD44 axis. Leukemia. 2014;28(4):853–864.

14. Pierre-Louis O, Clay D, Brunet de la Grange P, et al. Dual SP/ALDH functionalities refine the human hematopoietic Lin-CD34+CD38- stem/progenitor cell compartment. Stem Cells. 2009;27(10):2552–2562.

15. Saland E, Boutzen H, Castellano R, et al. A robust and rapid xenograft model to assess efficacy of chemotherapeutic agents for human acute myeloid leukemia. Blood Cancer J. 2015;5(3):e297.

16. Challen GA, Little MH. A side order of stem cells: the SP phenotype. Stem Cells. 2006;24(1):3–12.

17. Svirnovski AI, Shman TV, Serhiyenka TF, Savitski VP, Smolnikova VV, Fedasenka UU. ABCB1 and ABCG2 proteins, their functional activity and gene expression in concert with drug sensitivity of leukemia cells. Hematol Amst Neth. 2009;14(4):204–212.

18. Imrichova D, Messingerova L, Seres M, et al. Selection of resistant acute myeloid leukemia SKM-1 and MOLM-13 cells by vincristine-, mitoxantrone- and lenalidomide-induced upregulation of P-glycoprotein activity and downregulation of CD33 cell surface exposure. Eur J Pharm Sci. 2015;77:29–39.

19. Nieth C, Lage H. Induction of the ABC-transporters Mdr1/P-gp (Abcb1), mrpl (Abcc1), and bcrp (Abcg2) during establishment of multidrug resistance following exposure to mitoxantrone. J Chemother. 2005;17(2):215–223.

20. Eppert K, Takenaka K, Lechman ER, et al. Stem cell gene expression programs influence clinical outcome in human leukemia. Nat Med. 2011;17(9):1086–1093.

21. Ng SWK, Mitchell A, Kennedy JA, et al. A 17-gene stemness score for rapid determination of risk in acute leukaemia. Nature. 2016;540(7633):433–437.

22. Birbrair A, Frenette PS. Niche heterogeneity in the bone marrow. Ann N Y Acad Sci. 2016;1370(1):82–96.

23. Crane GM, Jeffery E, Morrison SJ. Adult haematopoietic stem cell niches. Nat Rev Immunol. 2017;17(9):573–590.

24. Wei Q, Frenette PS. Niches for Hematopoietic Stem Cells and Their Progeny. Immunity. 2018;48(4):632–648.

25. Arai F, Hirao A, Suda T. Regulation of hematopoietic stem cells by the niche. Trends Cardiovasc Med. 2005;15(2):75–79.

26. Gillet J-P, Gottesman MM. Overcoming multidrug resistance in cancer: 35 years after the discovery of ABCB1. Drug Resist Updat. 2012;15(1–2):2–4.

27. Balzano M, De Grandis M, Vu Manh T-P, et al. Nidogen-1 Contributes to the Interaction Network Involved in Pro-B Cell Retention in the Peri-sinusoidal Hematopoietic Stem Cell Niche. Cell Rep. 2019;26(12):3257-3271.e8.

28. De Grandis M, Mancini SJ, Aurrand-Lions M. In quest for leukemia initiating cells in AML. Oncoscience. 2018;5(1–2):9–10.

29. Hosokawa K, Arai F, Yoshihara H, et al. Function of oxidative stress in the regulation of hematopoietic stem cell-niche interaction. Biochem Biophys Res Commun. 2007;363(3):578–583.

30. Boyd AL, Aslostovar L, Reid J, et al. Identification of Chemotherapy-Induced Leukemic-Regenerating Cells Reveals a Transient Vulnerability of Human AML Recurrence. Cancer Cell. 2018;34(3):483-498.e5.

31. Moschoi R, Imbert V, Nebout M, et al. Protective mitochondrial transfer from bone marrow stromal cells to acute myeloid leukemic cells during chemotherapy. Blood. 2016;128(2):253–264.

32. Saygin C, Matei D, Majeti R, Reizes O, Lathia JD. Targeting Cancer Stemness in the Clinic: From Hype to Hope. Cell Stem Cell. 2019;24(1):25–40.

33. Varatharajan S, Abraham A, Karathedath S, et al. ATP-binding casette transporter expression in acute myeloid leukemia: association with in vitro cytotoxicity and prognostic markers. Pharmacogenomics. 2017;18(3):235–244.

34. Kolitz JE, George SL, Marcucci G, et al. P-glycoprotein inhibition using valspodar (PSC-833) does not improve outcomes for patients younger than age 60 years with newly diagnosed acute myeloid leukemia: Cancer and Leukemia Group B study 19808. Blood. 2010;116(9):1413–1421.

35. Cripe LD, Uno H, Paietta EM, et al. Zosuquidar, a novel modulator of P-glycoprotein, does not improve the outcome of older patients with newly diagnosed acute myeloid leukemia: a randomized, placebo-controlled trial of the Eastern Cooperative Oncology Group 3999. Blood. 2010;116(20):4077–4085.

36. Dean M, Hamon Y, Chimini G. The human ATP-binding cassette (ABC) transporter superfamily. J Lipid Res. 2001;42(7):1007–1017.

37. Sawicki E, Schellens JHM, Beijnen JH, Nuijen B. Pharmaceutical development of an amorphous solid dispersion formulation of elacridar hydrochloride for proof-of-concept clinical studies. Drug Dev Ind Pharm. 2017;43(4):584–594.

38. Robey RW, Pluchino KM, Hall MD, Fojo AT, Bates SE, Gottesman MM. Revisiting the role of ABC transporters in multidrug-resistant cancer. Nat Rev Cancer. 2018;18(7):452-464.

39. Wijaya J, Fukuda Y, Schuetz JD. Obstacles to Brain Tumor Therapy: Key ABC Transporters. Int J Mol Sci. 2017;18(12).

Figure legends

Figure 1: MSCs from HDs or from AML patients confer a better survival to leukemia blasts, even in the presence of chemotherapy agents

Histogram **A** left panel represents the number of living AML blasts after a 3-day culture without MSCs (median 51 655 (56 830)) or with MSCs from healthy donors (HDs) (median 91 815 (94 556) or AML patients (median 56 896 (102 863)). Right panel represents the same conditions but in presence of 50nM of mitoxantrone. Culture conditions in presence of the different types of MSCs significantly confer a better survival to AML blasts ($p=0.0004$ for left panel and $p=0.0003$ for right panel, $n>10$, represents the number of AML blasts/MSC donor combinations). Histogram **B** shows fluorescence intensity of AML blasts stained with mitoxantrone after a 3-day culture with or without MSCs from HDs (one representative experiment on the 6 performed). Control (CT) represents non-stained blasts. Graph **C** represents mitoxantrone MFI in AML blasts cultivated (median 2191 (2032)) or not (median 3676 (3546)) on HD MSCs ($p=0.01$, $n=6$, Wilcoxon test). Graph **D** represents mitoxantrone MFI in AML blasts cultivated (median 3861 (1147)) or not (median 1821 (460)) on AML MSCs ($p=0.01$, $n=3$-9, Wilcoxon test).

Figure 2: Co-culture between AML blasts and MSCs modulates the ABC transporter functionality on leukemia blasts in a patient-dependent manner

Histograms **A**, **B** and **C** represent the percentage of AML blasts that efflux specific probes (ABC transporter activity) after a 3-day co-culture on HD MSCs. ABC transporter activities were quantified using specific probes (Dioc2,3, Purpurin 18, CMFDA for ABCB1, ABCG2, ABCC1, respectively) as mentioned on the histograms. ABCB1 activity is significantly increased ($p=0.0059$, $n=9$, Wilcoxon test) by AML blasts after a 3-day co-culture on HD MSCs. Histograms **D**, **E** and **F** show the corresponding probe MFI in AML blasts; Dioc2,3

MFI is significantly decreased (p=0.02, n=9, Wilcoxon test) in blasts after coculture with HD MSCs. Histograms **G**, **H** and **I** represent the percentage of AML blasts that efflux specific probes after a 3-day co-culture on AML MSCs. Activity of the ABCB1, ABCG2 and CMFDA transporters was significantly increased (p=0.01, p=0.02 and p=0.008 respectively, n=3 without MSC and n=9 with AML MSCs, Wilcoxon test). Histograms **J**, **K** and **L** show the corresponding MFI in AML blasts. Purpurin 18 and CMFDA MFI are significantly decreased (p=0.01 and p=0.01 respectively, n=3 without MSCs and n=9 with AML MSCs, Wilcoxon test) in co-culture conditions.

Figure 3: Circulating leukemia blasts acquire a SP phenotype in contact with MSCs from HDs or AML patients through alpha4 integrin interaction

Cytograms **A** illustrate the gating strategy of AML blasts for cytometry analysis (top left panel) and SP visualization before co-culture (top right panel) and after a 3-day culture without (bottom left) or with (bottom right) HD MSCs. Graph **B** recapitulates the percentage of SP AML blasts before and after a 3-day co-culture on MSCs (either from HDs or AML patients) ($p<0.001$, n=27, Wilcoxon test). Graph **C** shows the percentage of SP AML blasts after co-culture with HD MSCs ($p<10^{-4}$, n = 8 to 33) or AML patients ($p<10^{-4}$, n = 8 to 35). Cytograms **D** show SP phenotype observed on AML blasts from MSC adherent (**left** panel) or supernatant fractions (SN, **middle** panel) and in transwell experiments (**right** panel) after a 3-day co-culture with HD MSCs. Graph **E** recapitulates the percentage of SP blasts in the 3 experimental conditions.

F and **G** show the percentage of SP AML blasts after co-culture or not with HD MSCs and after inhibition of beta 1 (n=18) and alpha 4 integrins (p=0.04, n=7) or CD44 (n=18) (**F)** and their downstream signaling pathways (**G)** using Dasatinib, LY294002, CAS2859863 and

LY209031, inhibiting Src (p=0.002, n=9), AKT (p=0.003, n=9), STAT5 (p=0.009, n=9) and GSK3 pathways (p=0.01, n=6) respectively.

Figure 4: The MSC-induced SP functionality in leukemia blasts is associated with quiescence and chemotherapy efflux through ABC transporter activation

Cytograms and histograms (**A**) show gating strategies and percentage of SP and MP blasts in G0 and in G1-S-G2-M after a 3-day co-culture on HD MSCs. Cell cycle status of SP *versus* MP blasts was analyzed adding pyronin Y during Hoechst staining. SP blasts are mostly in G0 (median 76% (16.5%)) compared to MP (median 33.45% (18.6%)) blasts which are in G1-S-G2-M (p=0.0009, n=12, Wilcoxon test). Transcriptomic analysis of SP blasts compared to MP blasts is shown in panel **B**. Cytograms **C** show gating strategy to evaluate mitoxantrone efflux in SP or MP blasts. Quantification of mitoxantrone MFI (**D**) in SP (median 1584 (1845)) and in MP (median 3219 (1706)) blasts (p=0.0052, n=12, Wilcoxon test). Graph **E** shows DioC2,3 MFI evaluating ABCB1 activity in SP (median 239 (4056)) and MP cells (median 1298 (5418)) (p= 0.023, n=7, Wilcoxon test).

Figure 5: The SP functionality of AML blasts induced by MSC interactions is associated with chemoresistance

Graph **A** shows the survival rate of SP (median 0.98 (0.46)) or MP (median 0.95 (0.24)) blasts after a 3-day co-culture with MSCs in presence of mitoxantrone (p=0.041, n=30, Wilcoxon test). Graph **B** shows the survival rate of SP or MP blasts after a 3-day co-culture with MSCs from HDs or AML patients. Graph **C** shows the absolute number of human SP and MP blasts in the femur of PDX mice after a 5-day treatment with either PBS or cytarabine (30mg/kg) (n= 3 mice per patient). Graph **E** represents the percentage of blasts that efflux mitoxantrone with or without verapamil after a 3-day co-culture on AML MSCs (p=0.05, n=5, Wilcoxon

test) and graph **F** shows the corresponding mitoxantrone MFI in AML blasts (p=0.05, n=5, Wilcoxon test). Graph **G** shows the number of living blasts co-cultivated on AML or HD MSCs after a 24h of mitoxantrone and treatment with or without verapamil (p= 0.01, n=6, Wilcoxon test)

Figure 6: SP blasts exhibit a detoxification program signature

Gene set enrichment analysis with transcriptomics data of sorted SP and MP blasts after a 3 day-co-culture on HD MSCs shows an up-regulation in SP cells of genes of xenobiotic metabolism and drug metabolism through the cytochrome P450 or other enzymes (**A**), an up-regulation in MP blasts of genes of oxidative phosphorylation, fatty acid metabolism and reactive oxygen pathway (**B**) as well as of genes from the reported stem cell signatures by Eppert *et al* and Ng *et al.* (**C**).

Figure 1

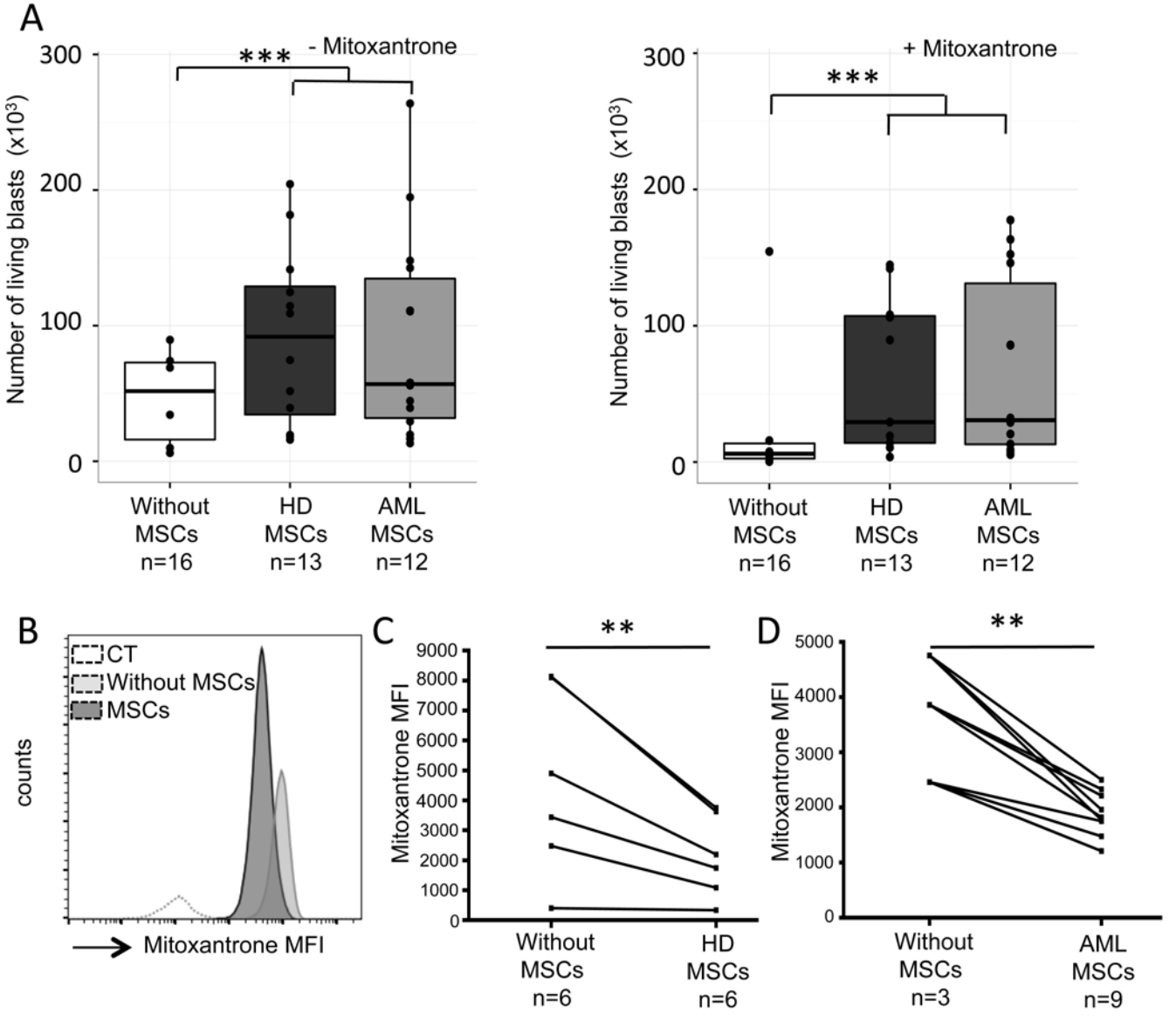
A
- Mitoxantrone
***
Number of living blasts (x10³)
300
200
100
0
Without MSCs n=16
HD MSCs n=13
AML MSCs n=12
+ Mitoxantrone
***
Number of living blasts (x10³)
300
200
100
0
Without MSCs n=16
HD MSCs n=13
AML MSCs n=12
B
CT
Without MSCs
MSCs
counts
Mitoxantrone MFI
C
**
Mitoxantrone MFI
9000
8000
7000
6000
5000
4000
3000
2000
1000
0
Without MSCs n=6
HD MSCs n=6
D
**
Mitoxantrone MFI
5000
4000
3000
2000
1000
0
Without MSCs n=3
AML MSCs n=9

Figure 2

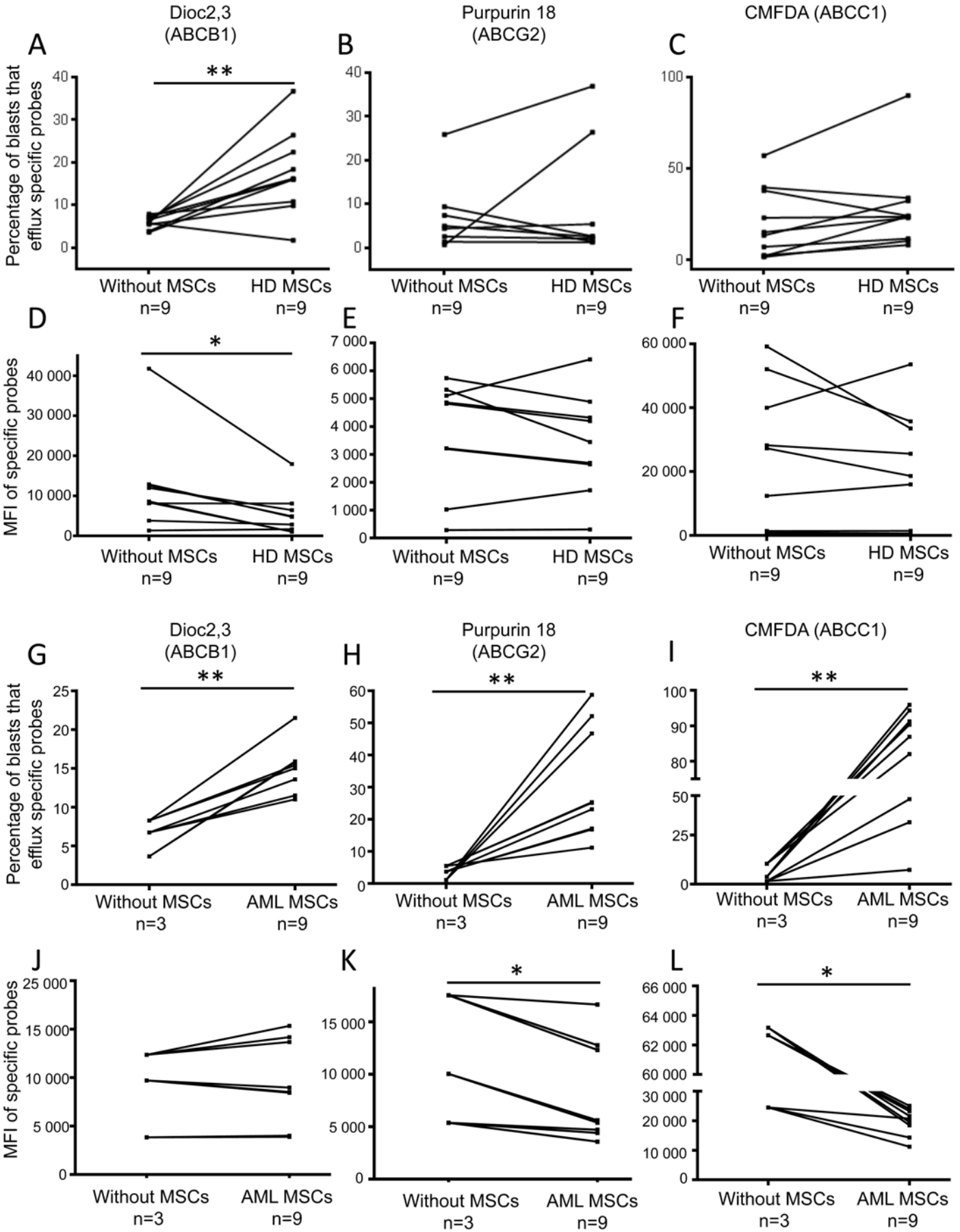
Dioc2,3
(ABCB1)
Purpurin 18
(ABCG2)
CMFDA (ABCC1)
A
B
C
D
E
F
G
H
I
J
K
L
Percentage of blasts that efflux specific probes
MFI of specific probes
**
*
Without MSCs
n=9
HD MSCs
n=9
Without MSCs
n=3
AML MSCs
n=9

Figure 3

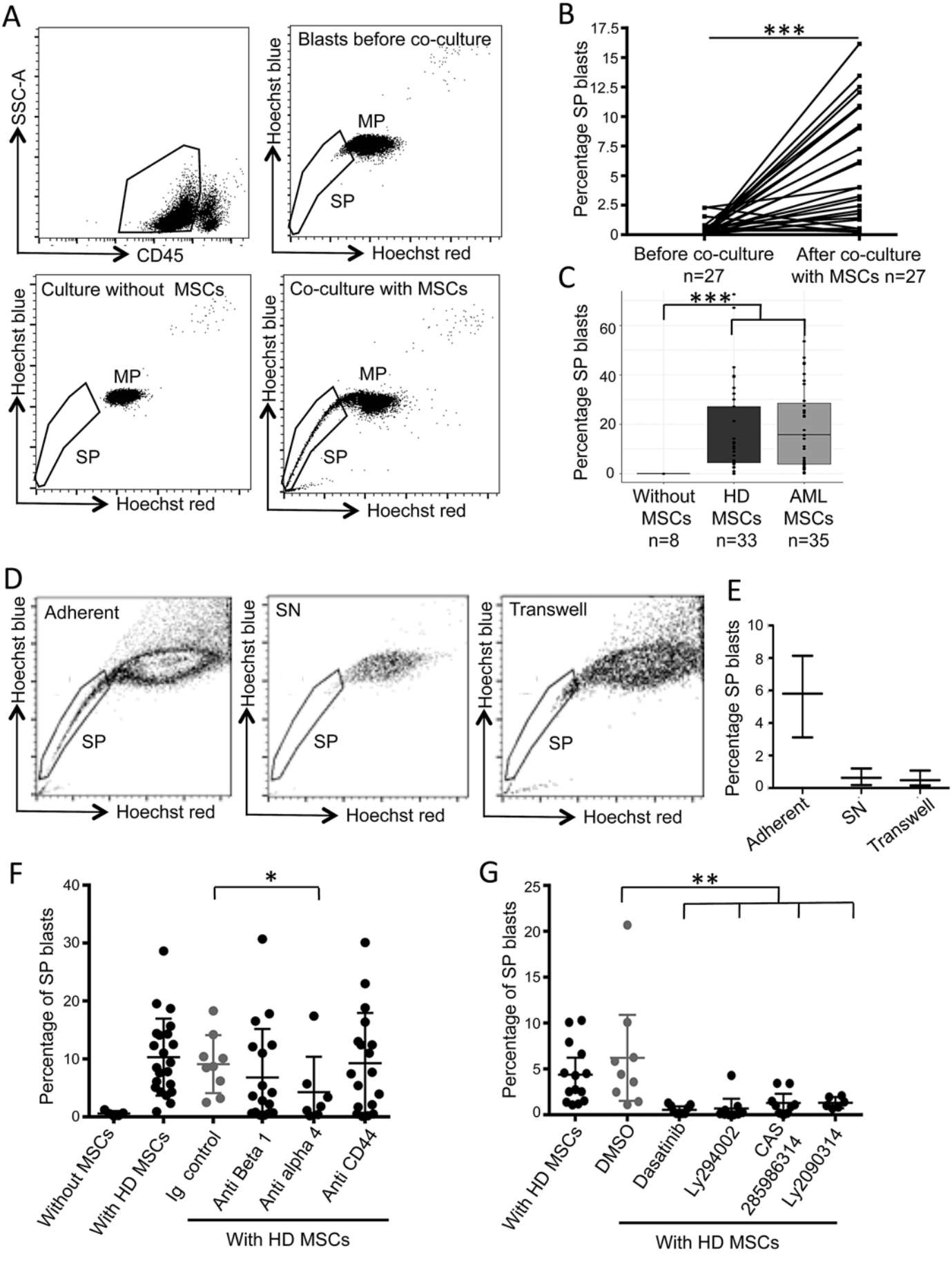
A
SSC-A
CD45
Blasts before co-culture
Hoechst blue
Hoechst red
MP
SP
Culture without MSCs
Co-culture with MSCs
B
Percentage SP blasts
***
Before co-culture n=27
After co-culture with MSCs n=27
C
Without MSCs n=8
HD MSCs n=33
AML MSCs n=35
D
Adherent
SN
Transwell
E
Adherent
SN
Transwell
F
Percentage of SP blasts
*
Without MSCs
With HD MSCs
Ig control
Anti Beta 1
Anti alpha 4
Anti CD44
With HD MSCs
G
**
With HD MSCs
DMSO
Dasatinib
Ly294002
CAS 285986314
Ly2090314
With HD MSCs

Figure 4

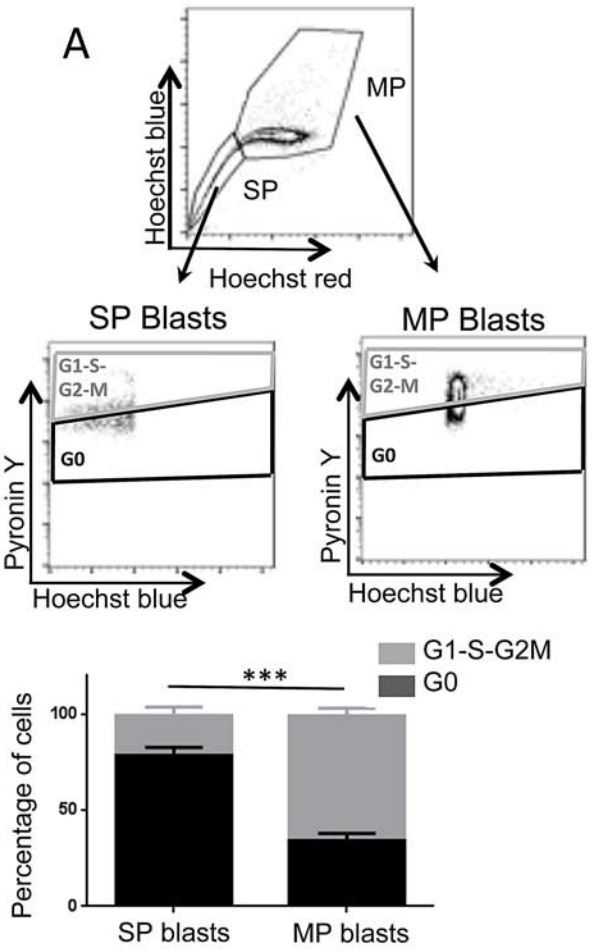

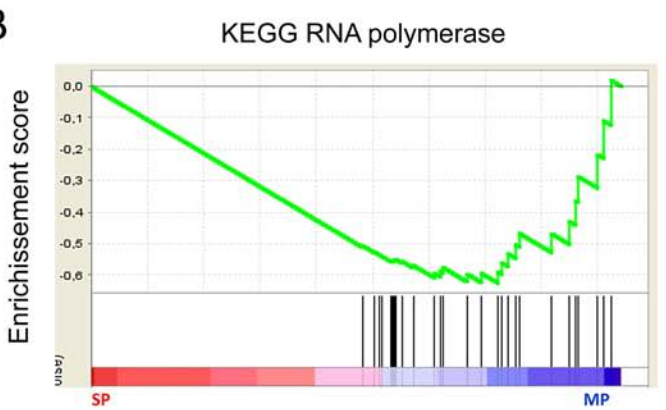

Gene Set Kegg	NES	P-value
Nucleotide excision repair	-2,65	< 0,0001
DNA replication	-2,28	< 0,0001
Mismatch repair	-2,08	< 0,0001
RNA degradation	-1,98	< 0,0001
RNA polymerase	-1,8	< 0,0001
Cell cycle	-1,79	< 0,0001
Base excision repair	-1,65	< 0,0001

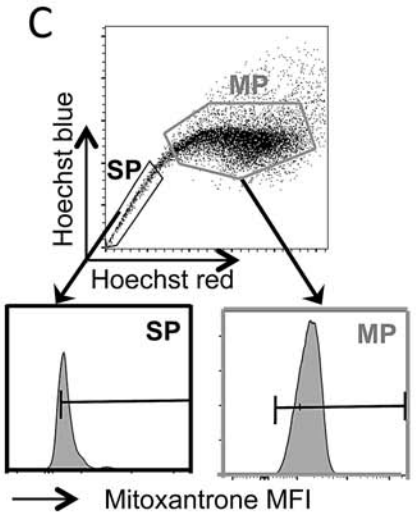

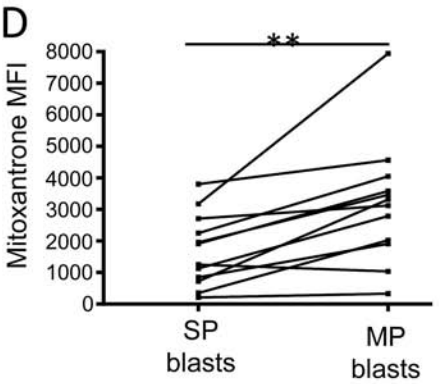

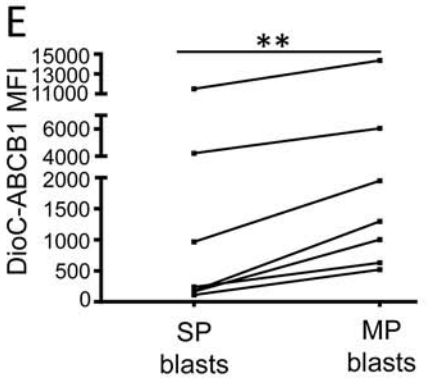

Figure 5

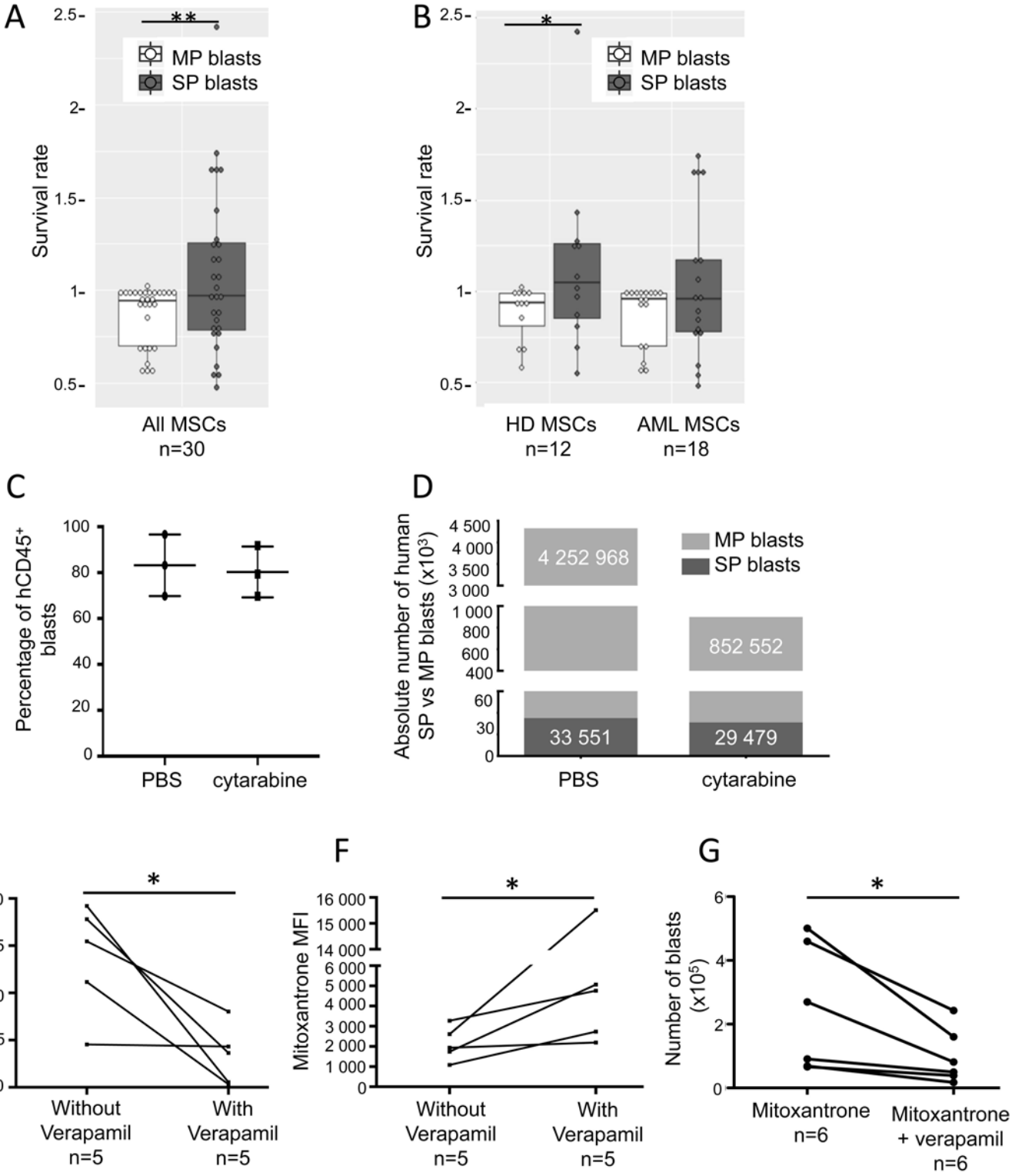
A
**
MP blasts
SP blasts
Survival rate
2.5
2
1.5
1
0.5
All MSCs
n=30
B
*
MP blasts
SP blasts
Survival rate
HD MSCs
n=12
AML MSCs
n=18
C
Percentage of hCD45+ blasts
100
80
60
40
20
0
PBS
cytarabine
D
Absolute number of human SP vs MP blasts (x10³)
MP blasts
SP blasts
4 252 968
852 552
33 551
29 479
PBS
cytarabine
E
*
Percentage of blasts that efflux mitoxantrone
Without Verapamil n=5
With Verapamil n=5
F
*
Mitoxantrone MFI
Without Verapamil n=5
With Verapamil n=5
G
*
Number of blasts (x10⁵)
Mitoxantrone n=6
Mitoxantrone + verapamil n=6

Figure 6

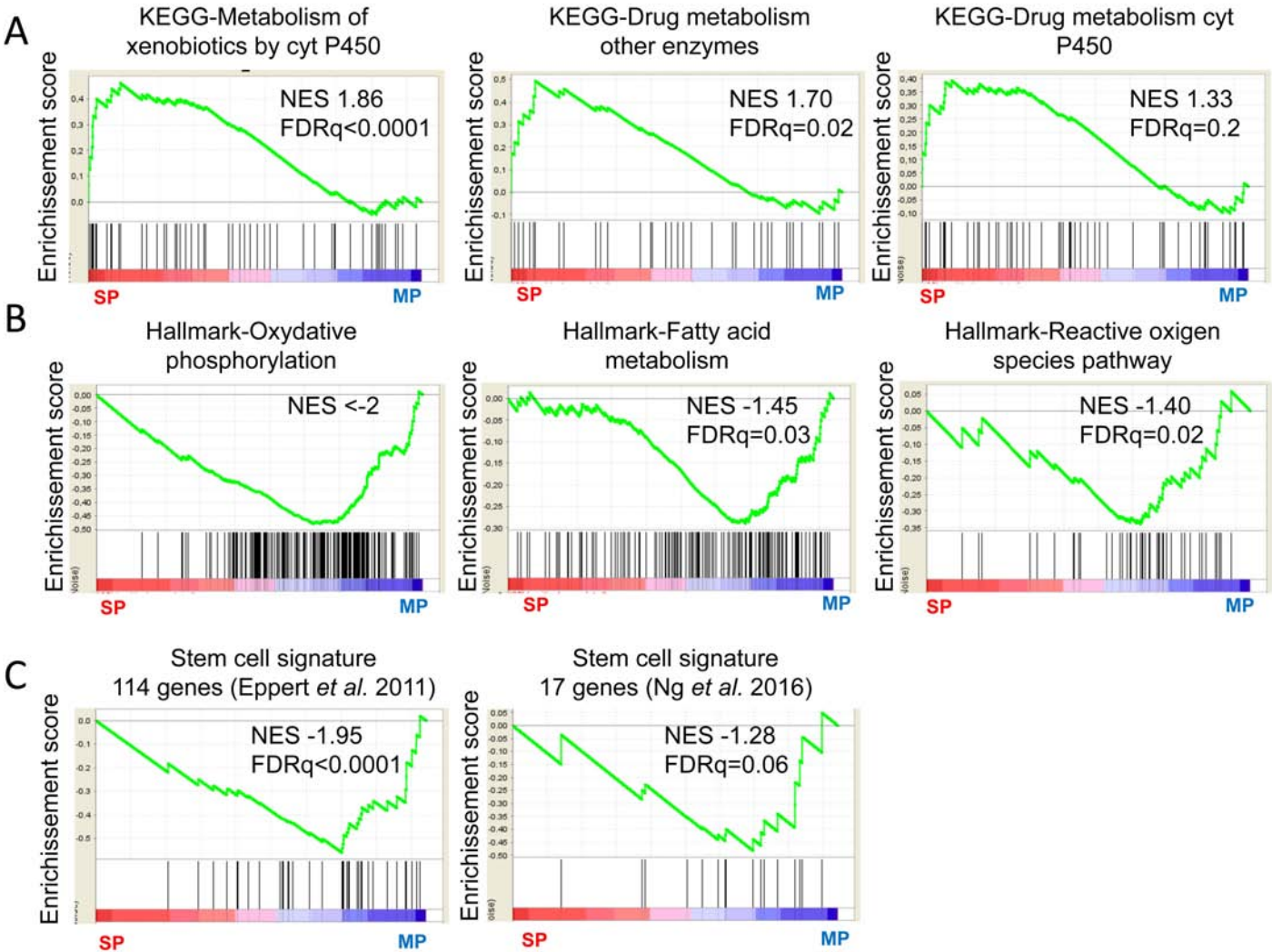
A
KEGG-Metabolism of xenobiotics by cyt P450
NES 1.86
FDRq<0.0001
KEGG-Drug metabolism other enzymes
NES 1.70
FDRq=0.02
KEGG-Drug metabolism cyt P450
NES 1.33
FDRq=0.2
B
Hallmark-Oxydative phosphorylation
NES <-2
Hallmark-Fatty acid metabolism
NES -1.45
FDRq=0.03
Hallmark-Reactive oxigen species pathway
NES -1.40
FDRq=0.02
C
Stem cell signature 114 genes (Eppert et al. 2011)
NES -1.95
FDRq<0.0001
Stem cell signature 17 genes (Ng et al. 2016)
NES -1.28
FDRq=0.06
Enrichissement score
SP
MP

Supplementary material

Isolation and culture of mesenchymal stromal cells

Bone marrow mononuclear cells (BM-MNC) were obtained from healthy donors (patient undergoing total hip replacement surgery at the polyclinic of Blois, France). BM-MNCs were counted using an automated cell analyzer (Sysmex) and seeded at 100.000/cm^2 in MEM alpha (Clinisciences) supplemented with 10% fetal bovine serum (FBS) and 10ng/mL of bFGF in order to amplify mesenchymal stromal cells (MSC).

AML MSCs were obtained from sample of bone marrow puncture carried out at diagnosis. AML bone marrow sample was seeded volume to volume in MEM alpha (Clinisciences) supplemented with 10% FBS and 10ng/mL of bFGF.

All MSCs were frozen in MEM alpha medium supplemented with 10% FBS and 10% DMSO (Sigma-Aldrich) for ulterior use.

Characterization of stromal cell

Human bone marrow mononuclear cells (BM-MSC) from healthy donors or AML MSCs were cultured in MEM alpha (Clinisciences) supplemented with 10% fetal bovine serum (FBS) and 10ng/mL of bFGF. Medium was replaced after 1 day and then every 3 days, each passage was done at 80% confluence using Trypsin-EDTA (Gibco). Then, MSCs were seeded at 4.000 MSCs/cm^2 for proliferation and 200 MSCs/25cm^2 for clonogenic tests (colony forming unit fibroblast (CFU-F)). Cultures were stopped when the cells were not able to achieve this level of confluence in 21 days. The growth characteristics of MSCs derived from AML patients and healthy donors were compared until the end of proliferation ability by expansion rate calcul. For CFU-F formation, the culture was stopped by ethanol fixation on day 10 and colored with

Crystal violet (Sigma-Aldrich). All MSCs were frozen in MEM alpha medium supplemented with 10% FBS and 10% DMSO (Sigma-Aldrich).

Osteogenic, adipogenic and chondrogenic differenciation of MSCs

For **osteogenic induction**, BM-MSCs and AML-MSCs were plated at $3x10^3$ cells/cm^2 in MEMα supplemented with 10% FBS, 0.1μM dexamethasone, 0.05 mM L-ascorbic acid-2-phosphate and 10mM β-glycerophosphate (Sigma-Aldrich, USA) for 21 days of culture. Medium was changed twice a week. Osteogenic cultures were stained histochemically for alkaline phosphatase detection using Abcys detection kit. Matrix mineralization was evaluated by 2% Alizarin Red (AR) (Sigma-Aldrich, USA).

Adipogenic differentiation was induced in BM-MSC and AML-MSC subconfluent cultures by 3 treatment cycles with induction media (DMEM supplemented 10% FBS and 1μM dexamethasone, 0.5mM 3-isobuthyl-1-methylxanthine (IBMX), 0.2mM indomethacin and 0.01mg/ml insulin (Sigma-Aldrich, USA)). Cycles were performed during 3-day induction culture and were followed by 1-3 days of maintenance culture in a maintenance medium (DMEM supplemented 10% FBS and 0,01mg/ml insulin) until day10. Between day 10 and day 21, cells were cultivated in maintenance medium refreshed twice a week. Adipogenic monolayer cultures were then histochemically stained with oil red O allowing lipid droplet detection (Cayman chemical, USA).

For **chondrogenic induction**, BM-MSCs and AML-MSCs were centrifuged at 500g for 5min without brake to form small pellets and cultured for 21 days in DMEM supplemented 10% FBS, 1mM sodium pyruvate, 0.17 mM ascorbic acid-2-phosphate, 10^{-7}M dexamethasone and 10ng/mL recombinant TGF-b3. After 3 weeks, cell pellets were resuspended with a graded series of ethanol treatment prior to being embedded in paraffin. Paraffin sections of 5 μm thickness were deparaffinized and stained with Alcian Blue.

Senescence assay

MSC cultures from primary AML cells and healthy donors were stained for β-galactosidase using senescence cells histochemical staining kit (Sigma-Aldrich) according to the manufacturer's specifications. Senescent stained cells were counted on photography using the ImageJ software.

Immunophenotyping of MSCs

Specific surface antigen expression was realized to characterize MSCs. MSCs were stained with anti-CD45 (clone J.33), anti-CD90 (clone F15-42-1-5), anti-CD105 (clone 1G2) anti-CD73 (clone AD2) (all from Beckman Coulter) and were analyzed using BD Fortessa apparatus (Beckon Dickinson) with Diva Software.

Transwell and neutralization experiments

For transwell experiments, AML blasts were cultivated in the upper chamber of a 3µm pore transwell laid on confluent HD MSCs.

For neutralization experiments, primary AML cells were incubated in SynH with anti-CD49d (α4), anti-CD44, anti-CD29 (β1) antibodies or their control immunoglobulins (Table S1). For inhibition of signal transduction pathways, inhibitors or vehicle controls were added to blast-MSC co-cultures (Table S1).

Table S1: Neutralizing antibody and inhibitor references and characteristics

Antibody/Inhibitor	Manufacturer	Clone	Concentration (µg/ml)
Anti-CD44	Progen	DF1485	1
Anti-CD49d (α4)	R&DSystems	2B4	20
Anti-CD29 (β1)	BD Biosciences	Mab13	1
Control IgG1	BD Biosciences		20
Control IgG2a	BD Biosciences	R-3595	1

Molecule	Pathway	Manufacturer	Concentration
Dasatinib	SRC	Cell Signaling	100nM
LY294002	AKT	Cell Signaling	10nM
CAS2859866314	Stat5	Millipore	50 µM
LY2090314	GSK3β	Sigma	1nM

SP cell detection and characterization

Hoechst staining was performed as previously described[1,2]. Briefly, 10^6 cells/ml were suspended in prewarmed (37° C) Dulbecco's modified Eagle's medium containing 2% FCS / 10mM HEPES / Hoechst 33 342 (final concentration: 5µg/10^6 cells/ml) and incubated at 37°C for 90 min.

Cell cycle analysis: Pyronine Y (50ng/ml; Sigma Aldrich) was added to the cell suspension during the last 15 min of Hoechst staining.

Transcriptomic analysis

After co-cultures and Hoechst staining, SP cells were sorted using FACSAria III SORP (BD Biosciences). Total RNAs were extracted using RNeasy microkit (Qiagen). Quantification of the RNA was performed on NanoDrop and its quality was assessed on Bio-analyzer 2100 (Agilent Technologies, CA). Transcriptome probes were synthetized starting with nucleic acid obtained from samples with RIN over 7, low quantity linear amplification was performed by following manufacturer instructions (Affymetrix, CA). Labeled probes were hybridized on Affymetrix HumanGene2.0ST microarray and scanned on Affymetrix station (Genom'IC, Cochin Institute facility). Microarray CEL files were normalized with Expression Console version 1.3 by RMA method (Affymetrix, CA). Gene set enrichment analysis (GSEA) was made with GSEA software version 2.2.0 with MSigDb database version 6.0[3]. Raw

transcriptome data were deposited on Gene Expression Omnibus (GEO) academic data repository under the access number GSE114633.

Patient-derived xenograft (PDX) model

Animals were used in accordance to a protocol reviewed and approved by the French Institutional Animal Care and Use (Committee of "Midi-Pyrénées" region-France). NOD/LtSz-scid/IL-2Rγchain^{null} (NSG) mice were produced at the Genotoul Anexplo platform of Toulouse (France) using breeders from Charles River Laboratory. NSG mice (6-9 weeks old) were sub-lethally treated with busulfan (30 mg/kg/day) 24 hours before intravenous injection of 1-10 × 10^6 leukemia cells in 200 µL of Hank's Balanced Salt Solution. Transplanted mice were treated with antibiotic (Baytril) for the duration of the experiment. Eight to 18 weeks after AML cell transplantation and when mice were engrafted (tested by flow cytometry on PB or BM aspirates), NSG mice were treated by daily intraperitoneal injection of either cytarabine (30 mg/kg; kindly provided by the pharmacy of the Toulouse University Hospital) or PBS for control mice, for 5 days. At the end of the 5 days, mice were killed and presence of SP cells was analyzed in the BM as described above.

References

1. Pierre-Louis O, Clay D, Brunet de la Grange P, et al. Dual SP/ALDH functionalities refine the human hematopoietic Lin-CD34+CD38- stem/progenitor cell compartment. Stem Cells 2009;27(10):2552–2562.
2. Malfuson J-V, Boutin L, Clay D, et al. SP/drug efflux functionality of hematopoietic progenitors is controlled by mesenchymal niche through VLA-4/CD44 axis. Leukemia 2014;28(4):853–864.
3. Subramanian A, Tamayo P, Mootha VK, et al. Gene set enrichment analysis: a knowledge-based approach for interpreting genome-wide expression profiles. Proc Natl Acad Sci USA 2005;102(43):15545–15550.

Table S2: Combination used to study ABC transporter functionality

MDR pump	ABCB1	ABCC1	ABCG2
Probes (Ex/Em)	$Dioc_2(3)$ (488/530)	CMFDA (488/530)	Purpurin 18
Provider	Molecular probes	Molecular probes	Santa Cruz
Concentration	5ng/mL	0,2µM	30µM
Viability marker	Sytox red	Sytox red	Iodure de propidium
CD45 (clone HI30, Sony)	CD45 APC-Cy7	CD45 BV421	CD45 FITC

A

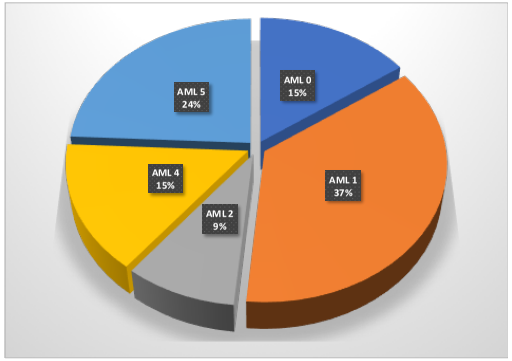

Figure S1

Figure S1: Patient information's

Graph **(A)** represents the distribution of AML subtypes used in the study. Table **(B)** gathers AML sample characteristics including the blast percentage evaluated at diagnosis by senior hemopathologists who reviewed each blood smear.

B

Patient number	Hospital	Gender	age	WHO	FAB	% of circulating blasts	Cytogenetic group	Karyotype	Molecular biology	Treatment	Evolution	Death
P1	Percy	F	26	aml with inv(16)	AML4Eo	30% - 41 %	fav	inv 16	rearrangement CBFbeta/MYH1	Daunorubicin + Aracytin	2 CR, 2 relapse	yes
P3	Percy	M	79	aml NOS	AML0	71%	unfab	monosomy 7 , Y deletion	not realized	Daunorubicin + aracytin, VIDAZA and then Amsacrin + Aracytin	1 CR, 1 relapse	yes
P5	Percy	M	60	aml NOS	AML5B	92%	int	monosomy 16	NPM1 non mut, FLT3 non mut	Idarubicin+ Aracytin (failure) then Azacitidin+ Gemtuzumab	1 CR, 1 relapse	yes
P6	Percy	F	56	aml with mutated NPM1	LAM4	27%	int	normal	NPM1 mut, WT1 over expressed	Daunorubicin + Aracytin puis Daunorubicin+ aracytin + mylotarg	1 CR, molecular relapse, CR2 and graft	no
P7	Percy	F	79	aml NOS	AML1	80%	unfav	complex monosomy 15 and 17	not realized	Daunorubicin + aracytin (failure) then Azacitidin	relapse	unknown
P10	Percy	M	75	aml NOS	AML1	18%	unknown	normal	not realized	Aracytin	CR	no
P12	Percy	M	45	aml NOS	AML2	15%	Int	normal	WT1 over expressed	Daunorubicin+ aracytin then mylotarg after 1st graft failure	graft, CR, relapse, graft, no remission	yes
P16	Percy	M	36	aml with biallelic mutation of CEBPA	AML1	65-90%	int	normal	WT1 over expressed CEBP alpha mut	daunorubicin + aracytin	CR	no
P17	Percy	M	65	aml with t(16;16)	AML4Eo	43%	fav	Inv 16	MYH11/CBFp +	Daunorubicin + aracytin (failure) then Aracytin + Mylotarg	relapse	yes
P19	Percy	M	67	aml with mutated NPM1	AML1	98%	int	trisomy 8	NPM1 mut , WT1 over expressed, tandem duplication Flt3	Daunorubicin + cytarabin	shock after treatment	yes
P21	Percy	M	76	aml with mutated NPM1	AML1	95%	int	normal	tandem duplication FLT3 , NPM1 mut	Daunorubicin + aracytin	CR	no
P23	Percy	M	62	aml NOS	AML5A	85%	int	Trisomy 8	FLT3 mut, WT1 over expressed	Daunorubicin + Aracytin(failure) then mylotarg + cytarabin	CR, relapse, CR, graft	no
P26	Percy	M	64	aml with mutated NPM1	AML1	82%	unfav	Trisomy 11	NPM1+ et WT1 over expressed +FLT3 mut, MLL	Daunorubicin + aracytin	graft, CR	no
P27	Percy	M	70	aml NOS	AML0	95%	int	Trisomy 13	not realized	Aracytin + Idarubicin	relapse	Yes
P28	Percy	F	76	aml NOS	AML5	90%	Int	normal	not realized	LD aracytin	refractory relapse	yes
P33	Percy	F	37	aml NOS	AML2	14%	Int	normal	wt1 over expressed	Daunorubicin + cytarabin then Aracytin	CR	no
P39	Percy	M	66	aml NOS	AML5b	75-85%	Int	normal	normal	Aracytin + Idarubicin	refractory relapse	yes
P41	Percy	F	75	aml NOS	AML5A	40%	Normal	normal	not realized	Vidaza	relapse	unknown
P42	Percy	F	34	aml with biallelic mutation of CEBPA	AML2	76%	fav	normal	CEBPa duble mut	3+7 Daunorubicin	unknown	yes
P44	Percy	F	53	aml with mutated NPM1	AML1	86%	int	normal	NPM1 mut FLT3 mut	3+7 idarubicin	relapse	Yes
P47	Percy	F	53	aml NOS	AML1	87%	unfav	deletion of 7	normal	3+7 idarubicin	relapse	yes
P48	Percy	M	66	aml with t(11;X)	AML0	31%	unfav	trisomy 18 t(11;X)	MLL	3+7 idarubicin	CR	no
P51	Percy	M	48	aml with mutated NPM1	AML5A	52%	int	normal	NPM1 mut FLT3 itd	3+7 daunorubicin	relapse	unknown
P52	Percy	M	74	aml with mutated NPM1	AML5A	53%	Int	inv 9 (constit)	NPM1 mut	3+7 idarubicin	CR	no
P53	Percy	M	50	aml with mutated NPM1	AML5A	77%	Int	normal	NPM1 mut	3+7 daunorubicin	CR	no
P57	Percy	F	57	aml with mutated NPM1	AML1	81%	int	X deletion	NPM1 mut FLT3 itd	3+7 idarubicin	CR	no
P61	Percy	M	61		AML1	53%	Int	normal	CEBPa simple mut	3+7 idarubicin	CR	no
P62	Percy	F	44	aml with mutated NPM1	AML5	54%	fav	normal	NPM1 mut	3+7 daunorubicin	CR	no
P67	Percy	M	79	aml with inv(16)	AML4	29%	fav	inv 16	not realized	Vidaza		
P55	St louis	M	89	aml NOS	AML1							
P56	St louis	F	44	aml NOS	AML4							yes
P58	St louis	F	24	aml NOS	AML0 bi		nc	complex, hyperdiploidy	del NR3C1, del CREBBP, del CDNK2a	3+7 daunorubicin + vindesin-dexa	CR	no
P59	St louis	M	57	aml with t(16;16)	AML4Eo		fav	inv16	CBFbeta-MYH11	3+7 daunorubicin	Death before CR (septic shock)	yes
P60	St louis	F	56	aml with mutated NPM1	AML1		fav	normal	NPM1 mut	3+7+Mylotarg	CR	no

Figure S2

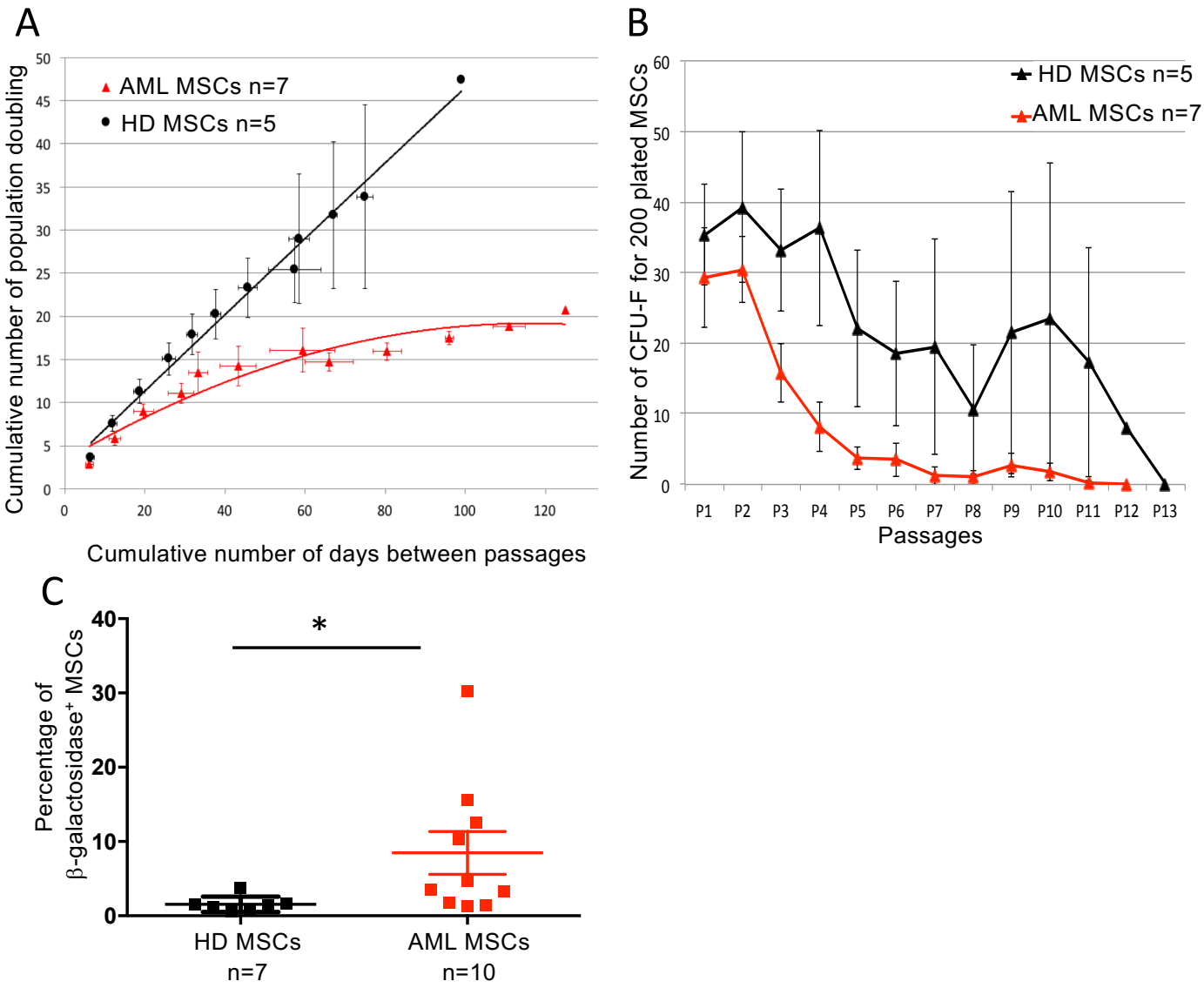

Figure S2: MSCs from AML patients exhibit a decreased expansion capacity and clonogenicity related to senescence

Graph **A** shows the expansion capacity of MSCs from HDs (black, n=5) or AML patients (red, n=7). The Cumulative number of population doubling for each kind of MSCs is represented per the cumulating number of days between passages. Graph **B** shows the clonogenicity of MSCs from HDs (black, n=5) or AML patients (red, n=7). The CFU-F number for 200 plated MSCs is represented for each cell passage. MSCs from AML patients exhibit a reduce clonogenicity compared to MSCs from HDs ($p<0,001$, n=5-8, Wilcoxon test). Graph **C** shows an increase of β-galactosidase$^+$ MSCs from AML patients (red, n=10) compared to MSCs from HD (black, n=7) at passage 4 ($p=0,018$ with Wilcoxon test).

Figure S3

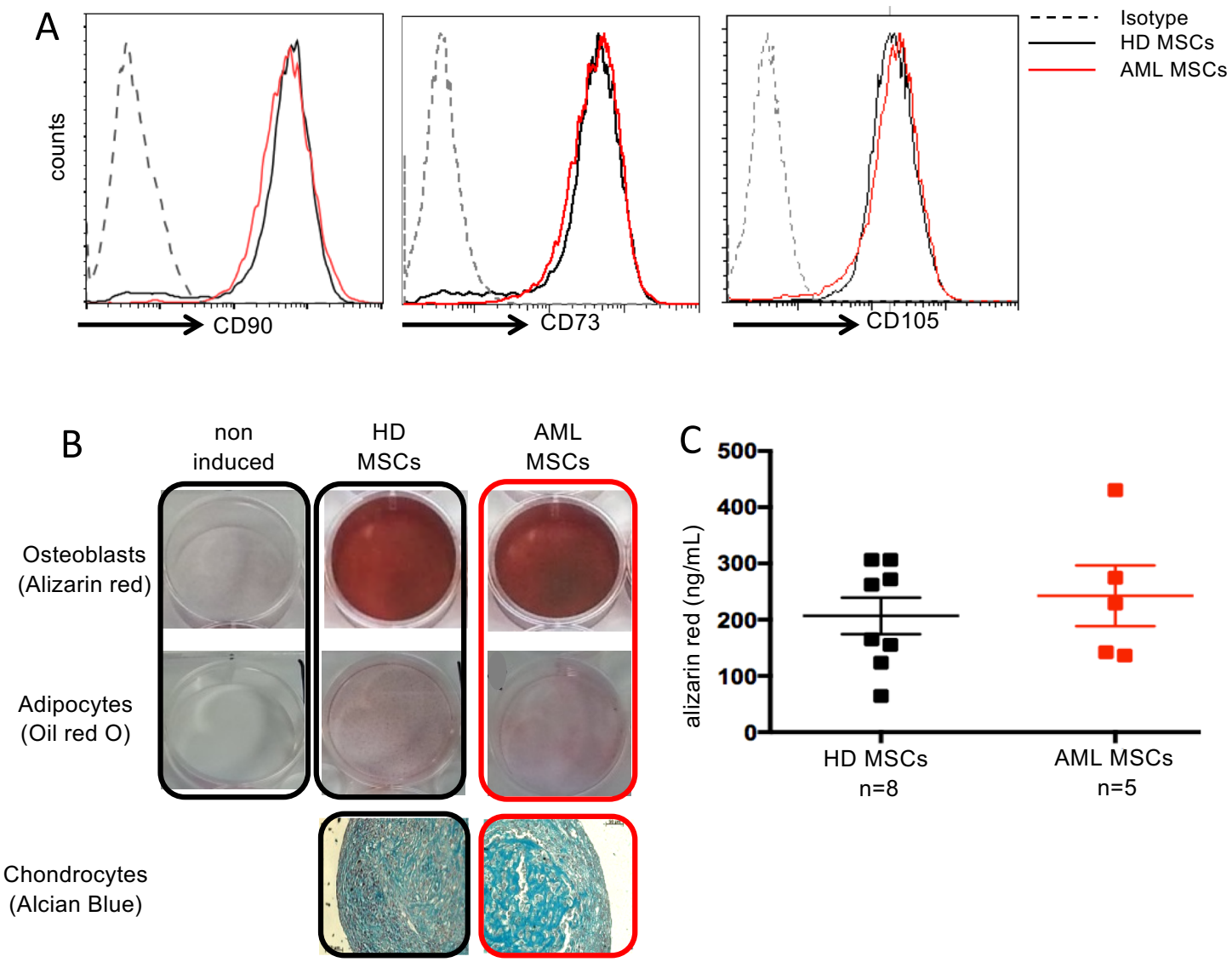

Figure S3: Characterization of MSCs from AML patients

Histograms **A** show FACS analyses of BM MSCs from HDs patients (black) and from AML patients (red) for CD90 and CD73 and CD105 antigens. MSCs from HDs or from AML patients were differentiated into osteoblasts, adipocytes and chondrocytes. Osteoblastogenesis was evaluated (**B**) and quantified (**C**) by alizarin red staining, adipogenenesis was evaluated by oil red O staining (**B**) and chondrogenesis was evaluated by Alcian blue staining (**B**).

Figure S4

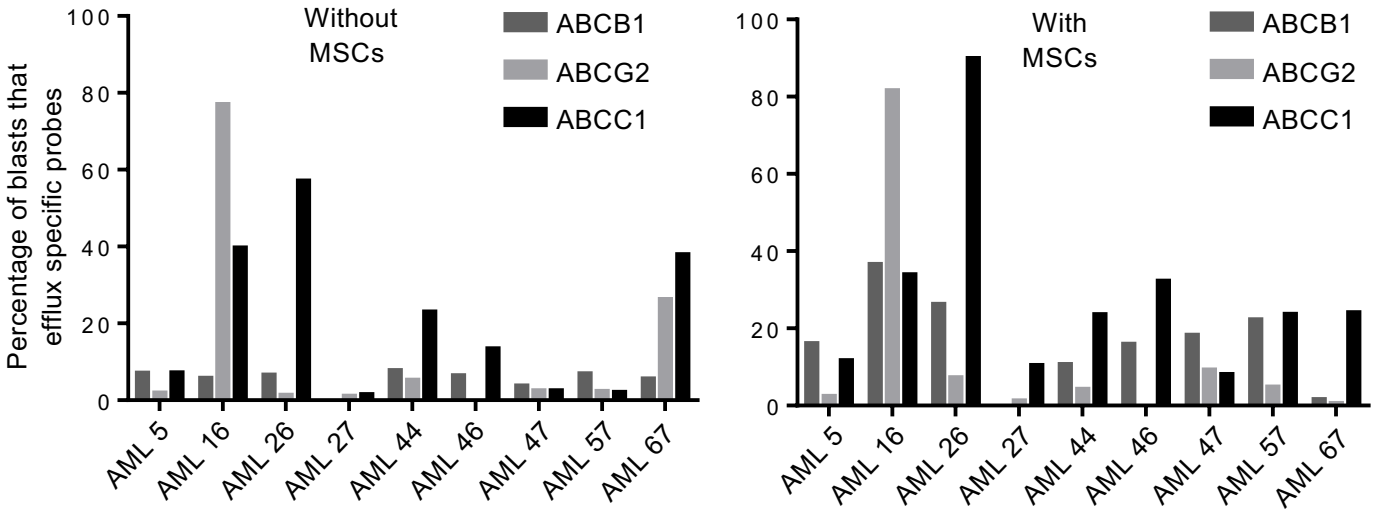

Figure S4: Analysis of Dioc2,3, Purpurin 18, CMFDA efflux by AML blasts patient per patient

Histogram shows the percentage of AML blasts that efflux specific probes (Dioc2,3, Purpurin 18, CMFDA for ABCB1, ABCG2, ABCC1, respectively), patient per patient, after a 3-day culture with or without MSCs from HDs.

Figure S5

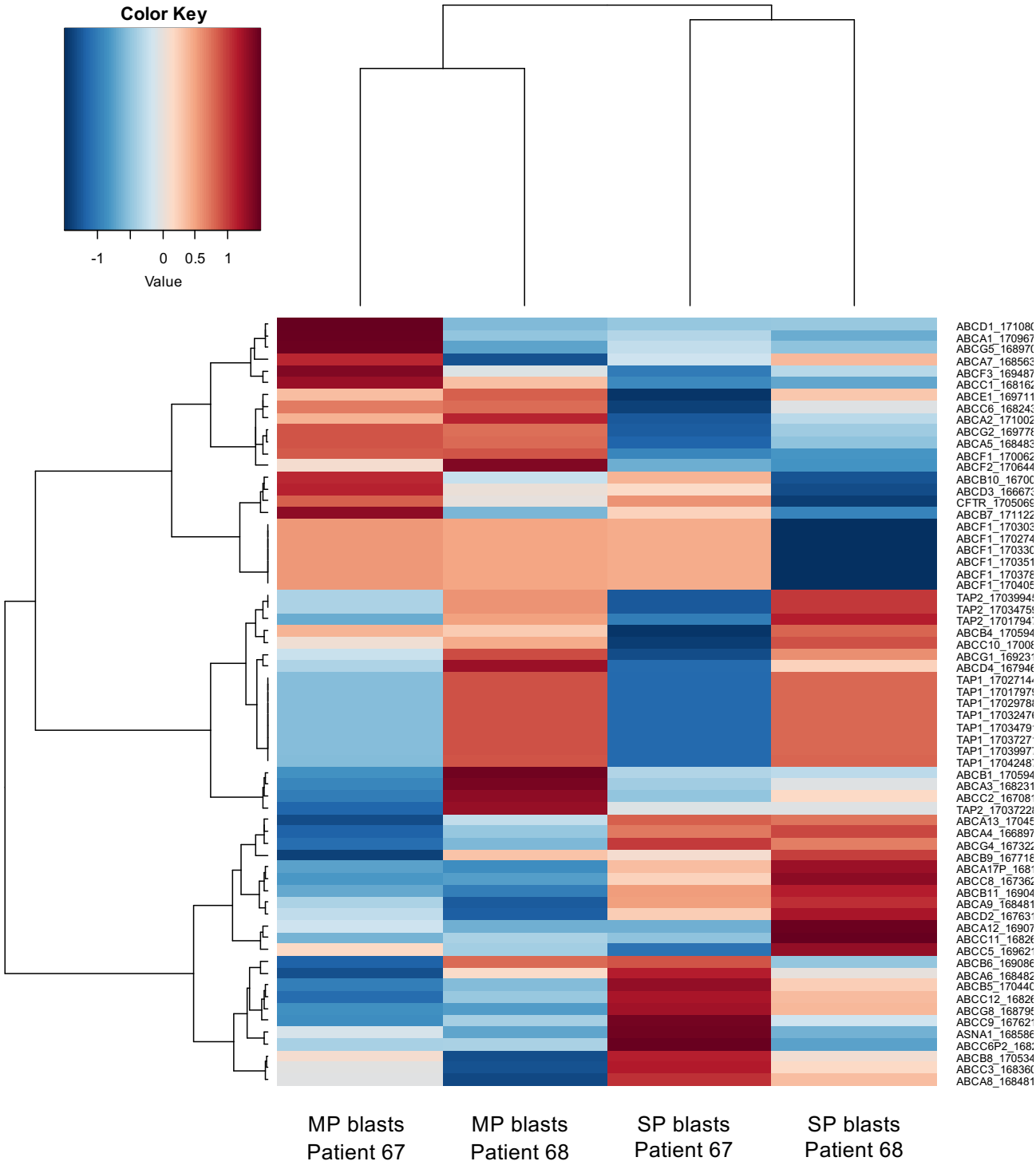

Figure S5: Transcriptomic analysis of ABC transporters in SP and MP from AML patients

Heatmap represents the expression level of ABC transporters obtained by transcriptomic analysis.

Figure S6

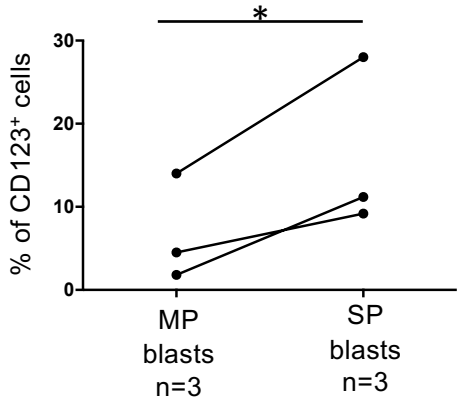

Figure S6: Quantification of CD123$^+$ cells in SP and MP blast population
Graph shows the percentage of CD123$^+$ blasts within the CD34$^+$ CD38$^-$ SP or CD34$^+$ CD38$^-$ MP populations (p=0,03 with paired t test, n=3).